Int. J. Nanoelectronics and Materials **2 No. 1** (2009) 75-89

2D-Modelling for the simulation of current-voltage characteristics in polysilicon schottky diode deposited by LPCVD and SAPCVD methods.

Nadia Benseddik[1,*], Mohammed Amrani[1], Zineb Benamara[1], Tayeb Mohammed-Brahim[2]

1) Laboratoire de Microélectronique, Faculté des sciences de l'Ingénieur, Université Djillali Liabès de Sidi-Bel-Abbès, 22000, Algeria.
2) Institut d'Electronique et de Télécommunication de Rennes1, Groupe Microélectronique, université de Rennes 1, Campus de Baulieu, F-35042, Rennes Cedex, France.

Abstract

The aim of this work is to compare the quality of the Schottky contact obtained between Silver and the un-doped polysilicon layer deposited on glass substrate (Corning 1737) by using two techniques: Lower Pressure Chemical Vapor Deposition LPCVD (LPCVD sample) and Sub Atmospheric Pressure Chemical Vapor Deposition SAPCVD (SAPCVD sample). A non ideal measured forward bias I-V characteristic has been observed. The electrical parameters are evaluated such as ideality factor (4.94 and 6.46), barrier height (0.57 eV and 0.60 eV), saturation current (6.74×10^{-3} mA and 2.14×10^{-2} mA) and series resistance (960Ω and 2300Ω), respectively on LPCVD and SAPCVD samples. Two-dimensional (2D) model of the I-V characteristics taking into account the localization of traps states in the grain boundaries is developed. We are also considered the U-distribution of traps states in the band gap. A good adjustment is obtained between measurement and simulation of the I-V characteristics and gives the energetic traps states distribution. The comparison of the performance of the two polysilicon layer deposition techniques have been analyzed and discussed. The experimental current curves are well fitted by this model which gives the energetic traps states distribution in the band gap. A good quality polycrystalline can be obtained using LPCVD technique but it is possible to deposit films with SAPCVD technique which it may be interesting candidate for the fabrication of solar cell.

1. Introduction

During recent years, polycrystalline silicon (poly-Si) is viewed as a very attractive material for thin film electronic devices. Research and development of poly-Si concentrate on two objectives: using the poly-Si thin film transistors (TFT's) in active matrix liquid crystal displays (AMLCD's) [1] and the development of the efficiency of solar cells by using the low-cost poly-Si thin films [2]. In both cases, the aim is to fabricate the devices on glass substrates. This choice limits the technological process to the temperature <600°C. In case of

*) For coresspondence, E-mail: n_benseddik@yahoo.fr

TFT and photovoltaic applications, the key factor for the attractiveness of poly-Si is to have a poly-Si material with large grain size [3, 4]. Unfortunately, according to the conditions during deposition, the polysilicon layers can consist of a random superposition of grains of different sizes, where, it appears a grains boundaries parallels and perpendiculars to the interface deposition. The interest of this paper is to understand the effect of the inter-granular traps states on the current transport in the Ag/Poly-Si/ITO/Glass substrate Schottky diode which the polysilicon is deposited at low temperature by two deposition techniques: low pressure chemical vapour deposition (LPCVD) and sub-atmospheric pressure chemical vapour deposition (SAPCVD) [5]. The advantage of this last is its use for applications that require a significant thicknesses such as PiN diode applied to the photovoltaic conversion of solar energy [6]. The performance of solar cells depends strongly on the combination of antireflective layer and collection grid. It has been reported that silver is the best choice for the grid instead of aluminium, because, Al diffuse more in the ITO or in the amorphous silicon silver [7]. The indium tin oxide (ITO) is deposited on rigid glass substrates because it is widely used as transparent conducting electrode [8]. The purpose of this work is firstly the electrical characterization of these structures using the I-V characteristics measurements, then, we develop a numerical code that interprets the current transport. In this model, we take into account the 2D effect of the geometrical model of the structure that consider the polysilicon film is assimilated by a succession of identical crystallites separated by grains boundaries [9], and assuming that the U-distribution of the energetic inter-granular traps states is shaped by the superposition of exponential and Gaussian distributions [10].

2. Technological part

Figure 1 gives the cross section of the studied sample.

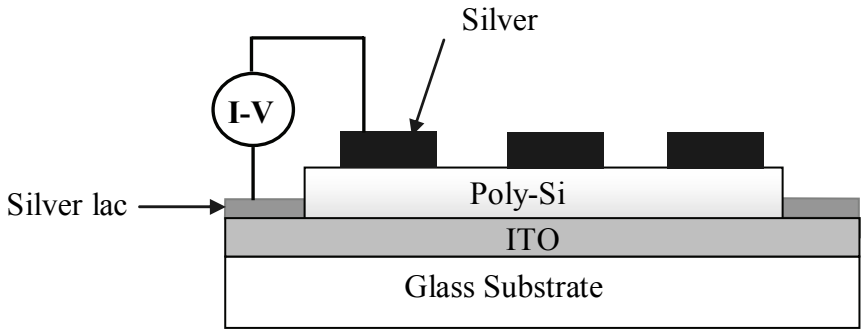

Fig. 1: Cross section of the studied Schottky diode

The structures have been elaborated with polysilicon thin films deposited on glass substrates Corning 1737 by two methods:

1. the first structure (LPCVD sample) is realized by the Low Pressure Chemical Vapor Deposition (L.P.C.V.D) process at 550 °C. The Raman analysis shows that polysilicon is deposited in amorphous state. Then, a thermal annealing at 600°C ensures a crystallization of the material;
2. the second structure (SAPCVD sample) is elaborated with polysilicon thin films deposited by the Sub Atmospheric Pressure Chemical Vapor Deposition (S.A.P.C.V.D). The temperature of the substrate is 557°C. The total pressure in the upper part is 100 mB, $aSiH_4$ gas flow of 0.05slm is used in the upper part of the reactor and H_2 flow 0.3slm in the lower one. The amorphous film is annealed at 600°C under vacuum for crystallization.

The two layers are un-doped where a thickness of films is set to 3μm. The sheet resistivity of polysilicon imposes the use of the highly conductive and transparent contact layer to collect photo-generated charge carriers, we use an Indium Tin Oxide (ITO) layer with a thickness of 1μm and a sheet resistance of about 25×10^{-4} Ω-cm. This layer serves as an antireflection coating [11]. Finally, to release a metallic gate, we have deposited by evaporation the silver layer with a diameter fixed to 1mm.

3. Current-Voltage (I-V) measurements and characterization:

Experimental I-V characteristics are evaluated by HP 4155B parameter analyser in dark chamber at 300 K. We plot in Figure 2 the I-V characteristics for LPCVD and SAPCVD samples.

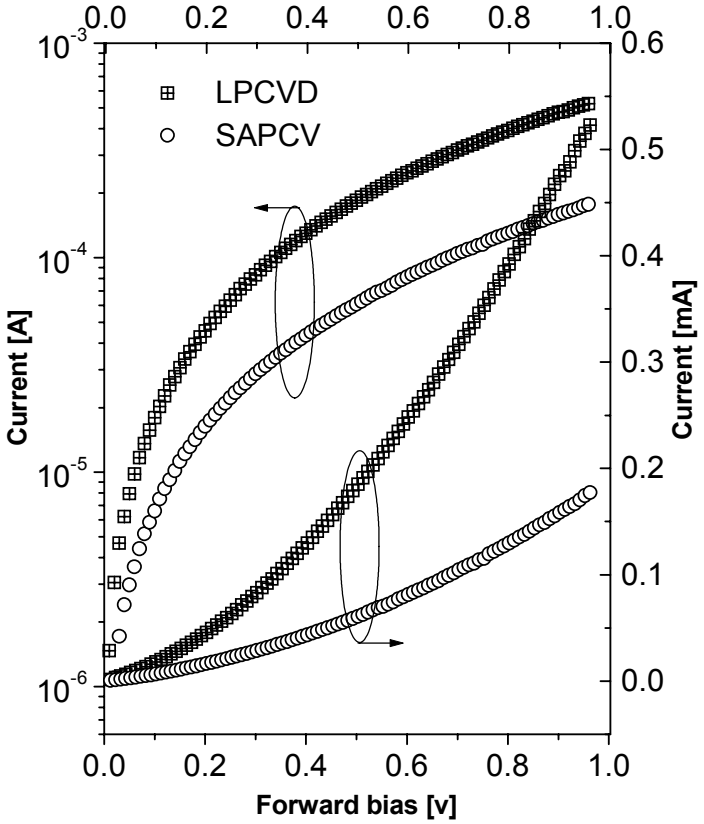

Fig. 2: Measured forward I-V characteristics of Ag/poly (Si) contact fabricated by LPCVD and SAPCVD methods.

By using the curves plotted on a linear scale, we observe that the current varies exponentially; consequently, the structures present a Schottky contact. By the semi-logarithmic scale, we observe a linear variation of I-V characteristics at low voltage (0-150mV). However, the applied voltage increases when the linearity of the ideal behavior deviates considerably. This result is due to the effect of diverse parameters such as inter-granular traps states N_T and series resistances R_S. To extract the barrier height, the ideality factor and the series resistances, we can use the method developed by Cheung and Cheung [12] based on the computation of the G and H functions defined by:

$$G(I) = \frac{dV}{d(Ln(I))} = \eta \frac{kT}{q} + RI \tag{1}$$

where η is the ideality factor, R is the series resistance, k is the Boltzmann's constant and T is the temperature.

$$H(I) = V - \eta \frac{kT}{q} Ln\left(\frac{I}{A A^* T^2}\right) \tag{2}$$

$$H(I) = \eta \phi_{bn} + RI \tag{3}$$

Here, A is the diode area (10^{-2} cm^{-2}), A^* is the effective Richardson constant (A^* =112 A K^{-2}) [13], and ϕ_{Bn} is the effective barrier height.

Theses functions correspond to another writing of the Schokley equation that assumes the forward bias I –V characteristics due to the thermoionic emission of the Schottky diode can be expressed as [14]:

$$I = I_s \exp\left(\frac{qV - IR}{\eta kT}\right) \tag{4}$$

where the saturation current I_s is given by:

$$I_s = AA^* T^2 \exp\left(-\frac{\phi_{Bn}}{kT}\right) \tag{5}$$

By using the functions G and H illustrated in Figure 3, we can gives the values of the ideality factor η , the series resistance R, the barrier height ϕ_{Bn} and the saturation current I_S summarized in Table 1.

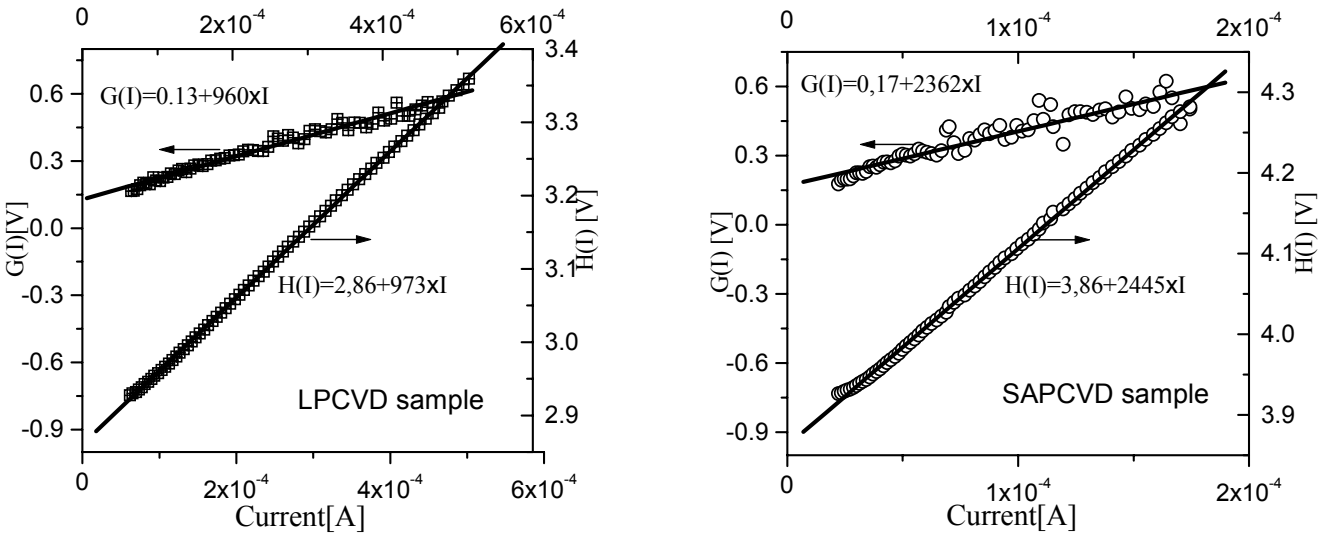

Fig. 3: illustration of the functions G and H allowing the calculation of η, R and ϕ_{Bn} .

Sample	η	R (Ω)	ϕ_{BN} (eV)	I_S (A)
LPCVD	4.94	960 by $G(I)$ 973 by $H(I)$	0.57	$2.14x10^{-5}$
SAPCVD	6.46	2362 by $G(I)$ 2445 by H(I)	0.60	$6.72x10^{-6}$

Table 1: Electrical parameters of Schottky diode Ag/poly-Si.

The results obtained in table 1 show that the samples LPCVD and SAPCVD present a weak current in the range of 0-1V, where the ideality factor increases from value of 4.94 for LPCVD sample to 6.46 for SAPCVD sample. This increase of η confirms that the current transport mechanism is the combination of the thermionic emission and the recombination phenomenon and the density of the traps states is more significant in SAPCVD sample than that LPCVD sample. We note that the series resistance for samples LPCVD and SAPCVD shows a larger value respectively 966Ω and 2403Ω. In our cases, the series resistance includes the lead resistance, the ohmic contact, and particularly the bulk resistance, which depends on the polysilicon resistivity. Concerning the effective barrier height, we observe that the obtained values are comparable to those obtained by C-V technique [15]. However, a difference in order 0.03 is examined for the effective barrier height between LPCVD and SAPCVD samples. This can be explained by the displacement of the free carriers in the layer which are constrained by the barriers heights, where the mobility decreases and the resistivity of the layer becomes significant.

4. Two-dimensional modeling

4.1. Physical model of the structure

In this section, we present the physical formulation of the current transport in polysilicon diode, where two-dimensional electrical model solves the Poisson's equation and the two carrier continuity equations:

$$-div(\varepsilon_s grad\phi) = q\left(p - n + N_D^+ - N_A^- + p_t - n_t\right) \tag{6}$$

Where ϕ is the electrostatic potential, ρ is the charge density, ε the dielectric constant, The n and p are the density of electron and holes, N_D^+, N_A^- are the doping concentrations, n_t and p_t are the concentrations trapped carriers of electrons in the acceptor states, and holes in the donor states, respectively.
To take into account trapping effects, the continuity equations can written by:

$$-\frac{1}{q} divJ_n = -U_n, \tag{7}$$

$$\frac{1}{q} divJ_p = -U_p \tag{8}$$

The current densities in the conduction and valence bands are expressed by the usual drift diffusion relations:

$$J_n = qn\mu_n E + qD_n grad(n) \tag{9}$$

$$J_p = q\mu_p pE - qD_p grad(p) \tag{10}$$

where μ_n, μ_p are the electrons and holes motilities, D_n and D_p are the carriers diffusivities and E the electric field. The contribution of the trapped charge to the electric potential is very important, especially when the polycrystalline silicon film is un-doped.

The concentrations n_t and p_t can be expressed as integrals of their respective energy distributions times the occupation probability:

$$n_t = \int_{E_V}^{E_C} y_A(E) P_A(E)\, dE \tag{11}$$

$$p_t = \int_{E_V}^{E_C} y_D(E)\left[1 - P_D(E)\right] dE \tag{12}$$

where y_A is the density of acceptor states per unit volume and energy, and P_A is the related occupation probability , similarly, y_D and P_D are the same quantities for donor states.

$$y_A(E) = y_{At}\, exp\left(\frac{E - E_c}{W_{At}}\right) + y_{Ad}\, exp\left(-\left(\frac{E - E_{Ad}}{W_{Ad}}\right)^2\right) \tag{13}$$

$$y_D(E) = y_{Dt}\, exp\left(\frac{E_v - E}{W_{Dt}}\right) + y_{Dd}\, exp\left(-\left(\frac{E - E_{Dd}}{W_{Dd}}\right)^2\right) \tag{14}$$

For an exponential tail distribution, the density of states (DOS) is described by its conduction and valence band edge intercept density (y_{At} and y_{Dt}) and by its characteristics decay energy (W_{At}, W_{Dt}).

For Gaussian distributions, the distribution of states is described by its total density of states (y_{Ad} and y_{Dd}) and by its characteristics decay energy (W_{Ad}, W_{Dd}).

As for the generation-recombination rate U, one finds [16]:

$$U = U_n = U_p = \int_{E_v}^{E_c} \left[y_A(E) \frac{\alpha_{nA}\alpha_{pA}np - e_{nA}e_{pA}}{\alpha_{nA}n + e_{nA} + \alpha_{pA}p + e_{pA}} + y_D(E) \frac{\alpha_{nD}\alpha_{pD}np - e_{nD}e_{pD}}{\alpha_{nD}n + e_{nD} + \alpha_{pD}p + e_{pD}} \right] dE \tag{15}$$

where e_{nA}, e_{pA}, e_{nD}, $e_{pD,}$ are the emission rates and α_{nA}, α_{pA}, α_{nD}, α_{pD} are the capture constants, respectively.

4.2 Geometrical model

The interface is located by the plan of equation X=0. For the region near to the interface (A-region), the polysilicon layer is assumed to be a successive identical monocrystallites separated by grain boundaries which are parallel and perpendicular to the interface [17]. In the grain boundaries with a thickness equal to 1nm [18], the energetic distribution of the trap states is the superposition of two exponential distributions and two Gaussian distributions of acceptor and donor type [19]. Far from the interface (B-region), the traps states are assumed distributed uniformly in the bulk [20]. Similarly, the energetic distributions of traps states are modeled by the superposition of two exponential and Gaussian distributions.Geometrically, these traps states are located only in grains boundaries of A-region and uniformly distributed in the bulk of B-region. The doping atoms with a concentration N_D are supposed all ionized at room temperature. The parameters simulation of the U-distribution of traps states in A-region (amorphous silicon parameters) and B-region (polysilcon parameters) are given in Table 2.

Parameters	*A- Region* in grains boundaries *a-Si [13,14,15]*	*B-Region* *poly-Si[16,17,18]*
Acc states characteristic energies (meV)	E_{At}=27. E_{Ad}=43	E_{At}=40. E_{Ad}=90
Don states characteristic energies (meV)	E_{Dn}=25. E_{Dd}=80	E_{Dn}=30. E_{Dd}=110
Acc states density at conduction band edge ($cm^{-3}eV^{-1}$)	$y_{At}=5\times10^{20}$, $y_{Ad}=5.10^{18}$	$y_{At}=8\times10^{19}$, $y_{Ad}=10^{17}$
Don states density at conduction band edge ($cm^{-3}eV^{-1}$)	$y_{Dt}=5\times10^{20}$, $y_{Dd}=5.10^{18}$	$y_{Dt}=8\times10^{19}$, $y_{Dd}=10^{17}$
Elec. (hole) capture cross-section of don. (acc.) states (cm^2)	$\sigma_{nD}=\sigma_{pA}=2.7\times10^{-15}$	$\sigma_{nD}=\sigma_{pA}=10^{-14}$
Elec. (hole) capture cross-section of acc. (don.) states (cm^2)	$\sigma_{nA}=\sigma_{pD}=10^{-15}$	$\sigma_{nA}=\sigma_{pD}=8.10^{-14}$
Electron band mobility (cm^2/Vs)	μ_n=13	μ_n=25
Hole band mobility (cm^2/Vs)	μ_p=67	μ_p=25
Decay energy Gaussian dist. of acc. and don. (eV)	$W_{GA}=W_{GD}$=0.42	$W_{GA}=W_{GD}$=0.3
Decay energy exponential tail dist. of acc. and don. (eV)	$W_{At}=W_{Dt}$=0.05	$W_{At}=W_{Dt}$=0.05

Table 2: List of parameters of traps states U-distribution used in the numerical simulation.

5. Simulation results and discussion

Before studying the effects of the simulation parameters on the I-V characteristic, we give in Fig.4 an example of variation of the electrostatic potential applied to the structure modeled previously. It is the result of the 2D solution of the system formed by the differential equations (6, 7 and 8). The system is solved by Gummel method where the detail of the numerical method used to solve the differential equation is given in reference [17, 20].

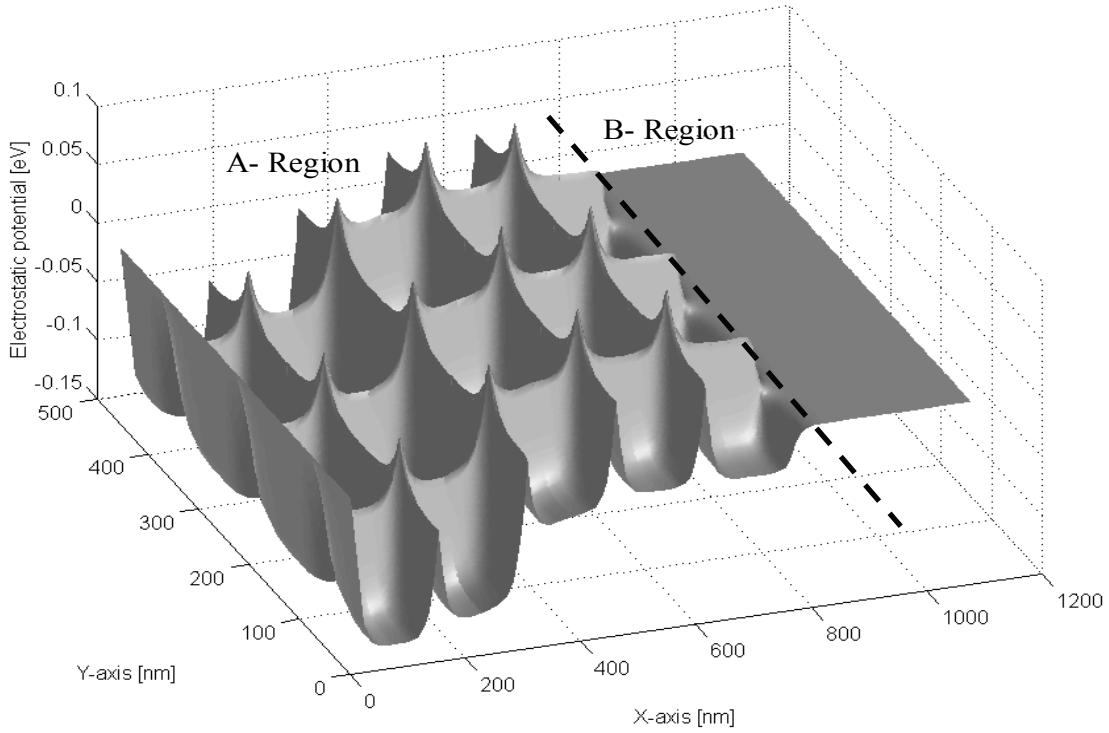

Fig. 4: Simulated electrostatic potential distribution in Ag-Poly(Si) structure, where : $N_D=2\times10^{17}$ cm^{-3}, the other parameters are those of illustrated in Table2.

In Figure 4, we observe that the variations of the electrostatic potential are similar in the grains except for those which are near to the interface where they can be affected by the first parallel grain boundary parallel [21,22]. At the intersection of the parallel and perpendicular grain boundaries, the potential is more significant and the barrier height reaches its maximum. The traps states density is sufficiently significant to allow the partial desertion of crystallite. The barrier height created in B-region represents approximately the average of those created by the grain boundaries of A-region.

To investigate the defects in polycrystalline silicon, we simulate the effect of two significant parameters in the characterization of polycrystalline materials: the doping concentration of the film N_D and the traps states distributions (n_t, p_t)

We trace in Figure 5 the evolution of I-V curves for doping concentrations range of 10^{17} and $10^{18}cm^{-3}$, where, the phenomenon of trapping is most effective. The parameters used in the numerical simulation are presented the table 2.

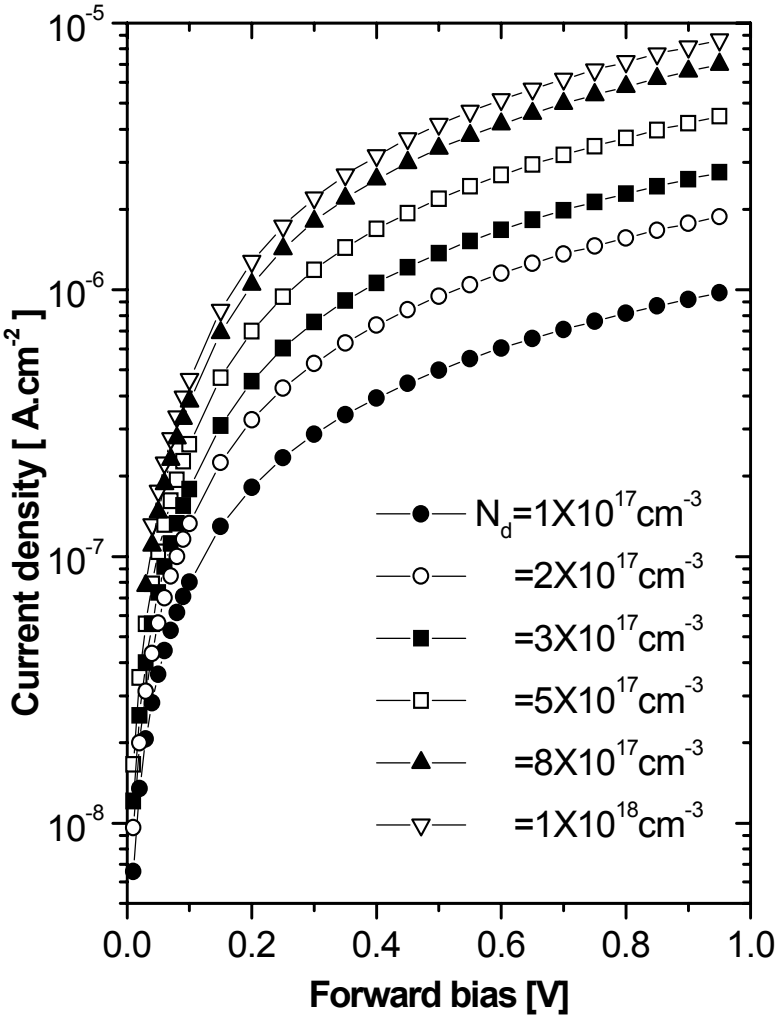

Fig. 5: Simulation of the doping concentration effect on the I-V characteristics.

In this figure we show that for any bias voltages, the variation of current increases when the doping concentration N_D increases. For strong injection, this increase is more significant. The ideality factor η improves from 2.71 to 4.22 when doping concentrations varies from 10^{17} to 10^{18}cm^{-3}, respectively. These values of η (higher than 2) confirm that the recombination current created in the space charge zone is added to the thermionic current. One the other hand, Figure 6 shows the effect of the traps states conduction band tail. From this figure, we can note a strong current increasing for low voltage due to higher trap densities, and a quasi-constant current in the range of high voltages, leading to an increase of series resistance. At low voltage, the recombination and diffusion process governs the conduction and enhanced with high trap densities. But the ideality factor varies in the low bias level range, from 1.38 to 5.21 which indicates that conduction is governed by recombination and the diffusion mechanisms even for low trap densities. No influence is observed in the low density range (< 10^{17} cm^{-3} eV^{-1}), due to the higher level range of doping ($8x10^{17}$ cm^{-3}).

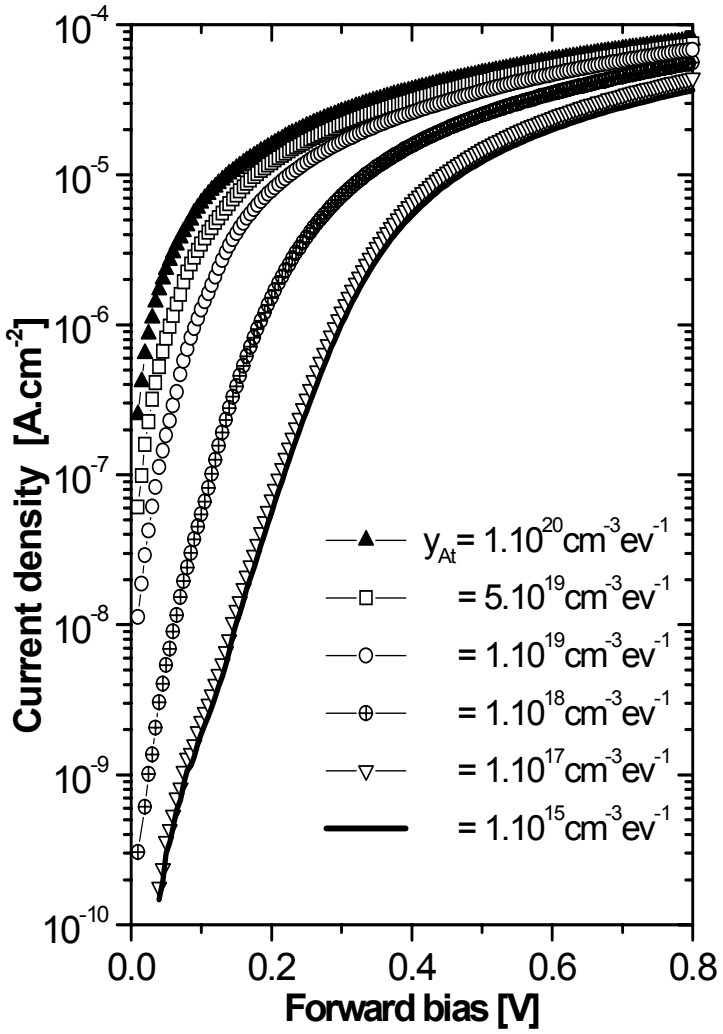

Fig. 6: Simulation of the effect of the traps states conduction band tail on the I-V characteristics.

For the densities y_{At} higher than 10^{18} $cm^{-3}.eV^{-1}$, we can deduce that the mechanism of recombination prevails. Higher than V= 0.2V, characteristic I(V) remains quasi-constant. It is dominated by the resistance series which increases when y_{At} increases. This resistivity is explained by the phenomenon of impoverishment of the polycrystalline layers creates by the trapping of the carriers.

Figure 7 shows the influence of the density y_{AD} of the dangling band on simulated characteristic I(V) whose contribution of the current density recombination is more significant since the dominant mid-gap defect is highly localized electronic state, commonly attributed to a silicon dangling bond, a site at which the silicon is three-fold-coordinated [23]. Therefore, the increase in density of states traps involves an increase of barrier height, which is also expressed in a lower mobility and a higher resistivity.

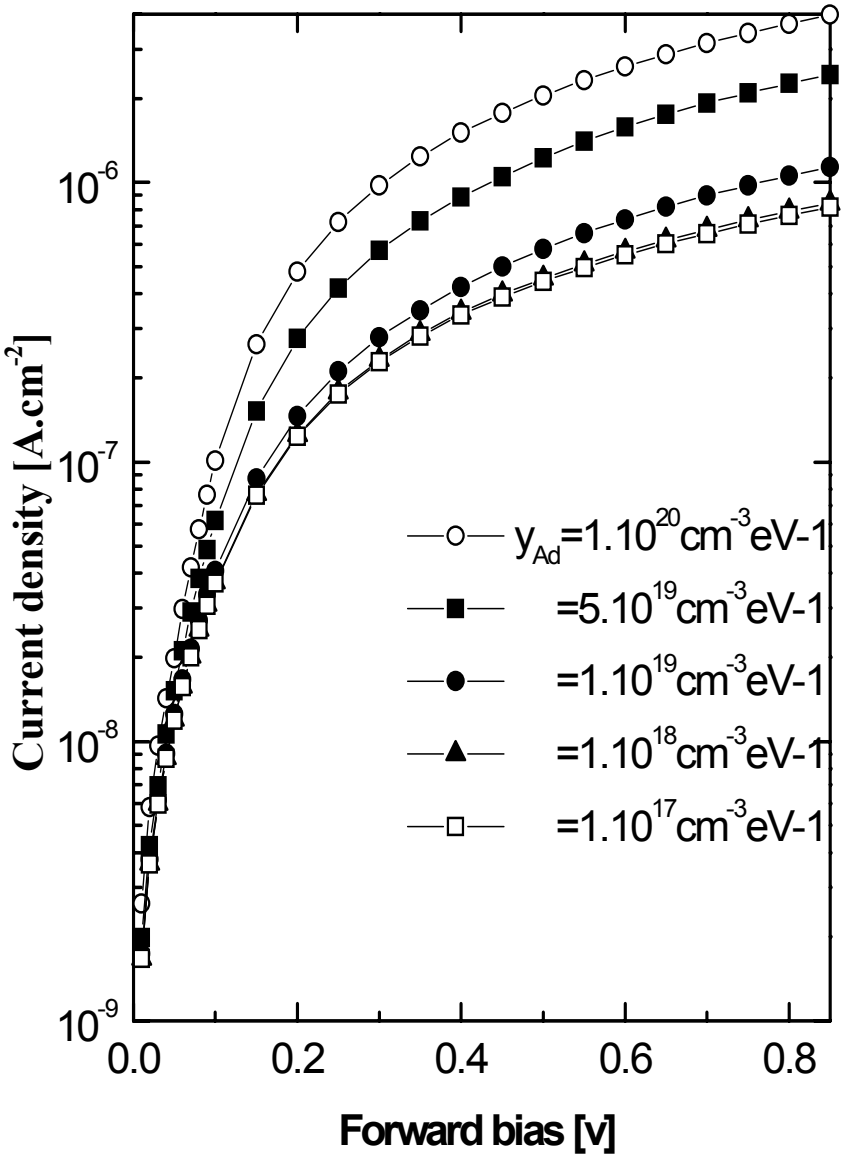

Fig. 7: Simulated effect of the dangling band acceptor state on the I-V characteristic.

The above simulated results allowed us to study the effect of the polysilicon physical parameters on the current transport in Schottky diode. As well as knowing the two layers are un-doped, we have measured the doping concentration by Hall Effect which the values are $5.10^{17}cm^{-3}$ and $10^{16}cm^{-3}$ for LPCVD and SAPCVD simples respectively.

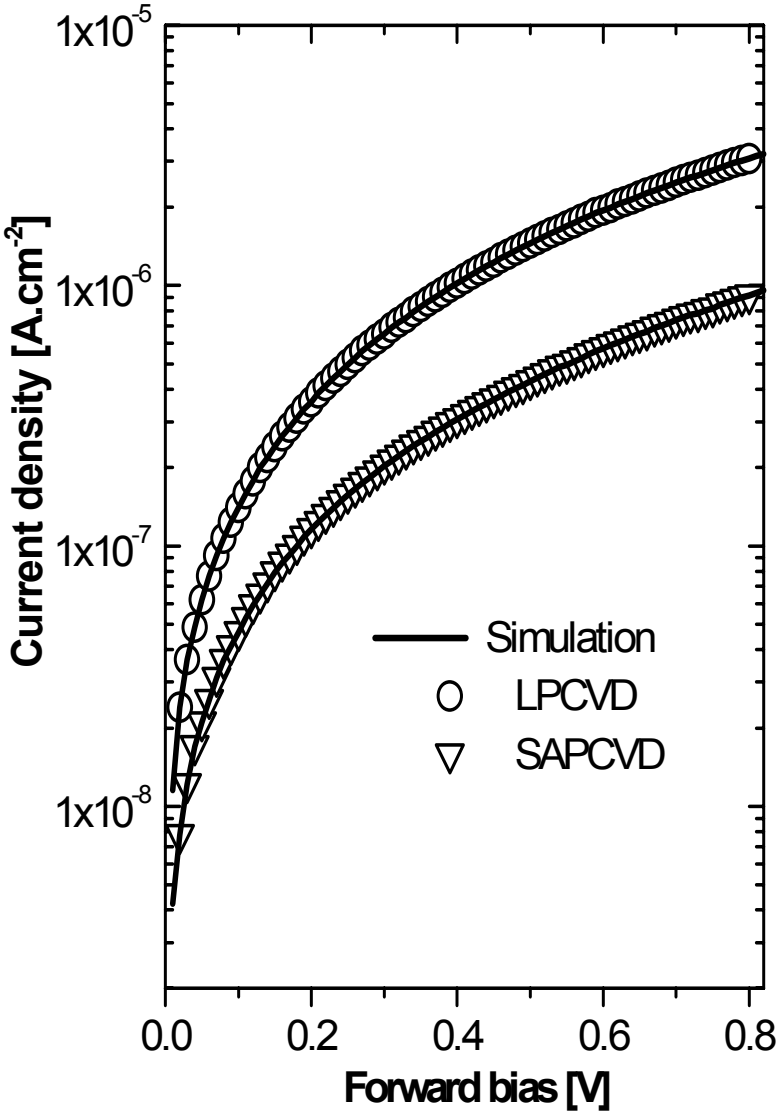

Fig. 8: Comparison between simulated and experimental I-V Characteristics and estimation of the distribution of traps states in A and B regions illustrated in figure 9.

From the usual physical parameters reported in the literature shown in the table 2 and these corresponding to technological process, the fit is obtained only from the adjustable trap states y_{Ad}, y_{At}, showing that the trap density effect strongly current level. As shown in the figure 8, we have well fitted the experimental curve of the structure LPCVD and SAPCVD of which the distribution of trap states extracted using the fitting are shown in figure 9.

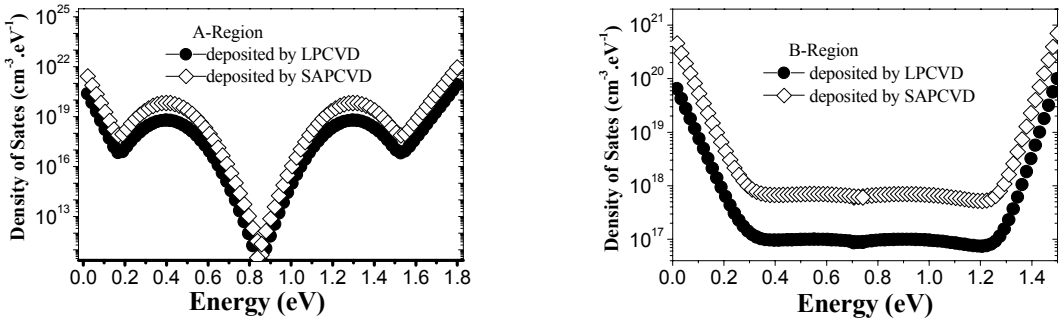

Fig. 9: The distribution of extracted traps states by using the fitting between simulation and experiment results.

(a): A-Region (in grains boundaries)
(b): B-Region (in bulk of B-region)

The distribution of the density of the states is confirmed by an experimental study obtained by Cao et al. [24] by using the field effect conductance method. From this figure, we can observe the mid-gap state density increased in A-region, while a constant mid-gap state density is examined in B-region. In addition, we note, that the values for samples deposited LPCVD are different from factor approximately of ten with the grain boundaries A-region (amorphous region), while a difference in a seven factor is examined in B-region (polycrystalline region). This can be explained by the increase in the temperature process which makes increase the dangling bonds [25]. A similar observation is reported by K. Pangal [26], who noted the increase in hydrogen content with decreasing growth temperature of which the density of dangling bonds is reduced. We can also observe that the distribution has been split into donor and acceptor traps at 43meV intervals such that the amorphous Fermi level is 0.85 eV in A-region and at 20 meV intervals such that the polysilicon Fermi level is 0.65 eV in B-region.

However, the values of density states for SAPCVD simple are estimated at y_{At}= 4×10^{20}cm^{-3}.eV^{-1} to 4×10^{21} cm^{-3}eV^{-1} and y_{Ad}=5×10^{19}cm^{-3} eV^{-1} to 7×10^{17}cm^{-3}eV^{-1}in A and B regions respectively. This result indicates that the good quality of polysilicon film can be obtained by using the LPCVD technique. These two shapes of the traps states density obtained in grains boundaries (amorphous) and polycrystalline regions are comparables to the results obtained by J. Dong et al. [27]. In This study, the comparison between electronic density of states DOS in the band-gap of amorphous and crystalline structures show that the crystalline structure has a defect free gap with sharp band edge, while the amorphous structure has extended bands tailing at both valence and conduction bands, as well as a few defect states in the middle of the band gap.

6. Conclusion

The aim of this work is to study experimentally and theoretically the current transport phenomenon in the undoped polysilicon Schottky diode deposited by two techniques: Low Pressure Chemical Vapor Deposition (LPCVD) and Sub Atmospheric Pressure Chemical Vapor Deposition (SAPCVD). Using the illustration of the function G, H deduced from the measurement of the I-V characteristics, we have determined the electrical properties of the structures and consequently we have deduced the following remarks:

- the values of the ideality factor and the series resistance (4.94 and 960 Ω for LPCVD diode and 6.94 and 2300 Ω for SAPCVD diode) confirm that the electric properties of structure deposited LPCVD are better than that deposited SAPCVD. These values which

are relatively higher are due principally to the contact metal-semiconductor and to the traps states contained in the grain boundaries.

- a small difference is observed between the effective barrier heights of the two structures (0.57 eV for LPCVD, 0.60eV for SAPCVD).

To explain these results, a two-dimensional (2D) code of current-voltage characteristics of polysilicon Schottky diode is developed. In this calculation, we consider that the polysilicon film is assimilated by a succession of identical crystallites separated by grains boundaries, and assuming that the U-distribution of the energetic inter-granular traps states is shaped by the superposition of exponential and Gaussian distributions.
This simulation program allows studying the effect of the physical and electrical parameters on the current transport in polycrystalline Schottky diode.

A good agreement is obtained between the experimental and simulated I-V characteristics of the two samples, where the corresponding traps states distribution of the two samples can extracted.

A good quality polycrystalline can be obtained using LPCVD technique but it is possible to deposit films with SAPCVD technique which it may be interesting candidate for the fabrication of solar cell.

References

[1] S. D. Brotherton, J. R. Ayres, M. J. Edwards, C. A. Fisher, C. Glaister, J. P. Gowers, D. J. McCulloch, and M. Trainor, Thin Solid Films **337**, 188 (1999).
[2] R. B. Bergmann, Appl. Phys. A **69**, 187 (1999).
[3] J.I Ohwada, M.Takabatake, Y.A. Ono, A. Mimura, N. Konishi, SID Dig, **131** (1989).
[4] I.W. Wu, A.G Lewis, T.Y. Huang and A. Chiang. IEEE Electron Device Lett 10, **123**, (1989)
[5] D. Maier - Schneider ,J Maibach, J . Micromech. Microeng **5**, 121 (1995).
[6] S. M. Fluxman, IEE Proc. Circuit Devices Syst, **141,** 56 (1994).
[7] P .Münster , M .Sarret, T. Mohammed - Brahim, and O. Bounnaud ,in 16 th European hotovoltaic Solar Energy Conference, Glasgow **634** (James & James ,2000).
[8] H. Kim, J. S. Horwitz, G. P Kushto, Z.H .Kafafi, D. B. Kressey, Appl. Phys. Lett.,**79**, 284 (2001).
[9] J.Y. Seto, J. Appl. Phys., **46**, 5247 (1975).
[10] T. Smaïl and Mohammed-Brahim, Philosophical Magazine B, **64**, 1925 (1991).
[11] A. Marmostein, A. T. Voutsas, R. Solanski, J. Appl. Phys., **82**, 4303 (1997).
[12] S. K. Cheung, N. W. Cheung. Appl. Phys. Lett. 85, **49** (1986).
[13] S. M. Sze Physics of semiconductor devices» 2 nd Edition Wiley and Sons Ed.New York 1981.
[14] K. Schroder, Semiconducteur Meterial and Device Characterization, NY: John Wiley & Sons (1998).
[15] M. Amrani, N. Benseddik, Z. Benamara, R. Menezla, M. Chellali, S. TiZi, T.Mohammed-Brahim, Journal of Materials Science and Engineering B,**121**, 71(2005).
[16] L. Colalong, M.Valdinoci, G. Baccarani, P. Migliorato and C. Reita, Solid-state Electronics **41**, 627 (1999).
[17] M. Amrani, Z. Benamara, R. Menezla , A . Boudissa, M . Chellali, T . Mohamed-Brahim, F. Raoult, J. Phys. D: App. Phys **38**, 596,(2005).
[18] J. Werner and M. Peisl, Physical Review B, **31**, 6881 (1985).
[19] J.R. Ayres, N. D . Young IEEE. Trans. Electron. Dev., **33**,141 (1994).
[20] M. Amrani, R. Menezla, H. Sehil, F. Raoult, H. Boudiaf, Z.Benamara, J. Mater. Sci. Eng. B, **49**,197 (1997).

[21] H. Lhermite, O. Bonnaud , Y. Colin, A. Mercier, IEEE trans. Electron. **28**, 675(1988).
[22] M. Amrani, H. Sehil, R. Menezla, Z. Benamara, F. Raoult, Solid Stat. Electron. **42**, 1925 (1998).
[23] S. Aljishi, Phys. Rev. Lett. **64**, 2811 (1990).
[24] M. H. Brodsky, M. Cardona, J. J. Cuomo, Phys. Rev. B 16, **8**,3556 (1977).
[25] M. Cao, T. S. King, K. C. Sarsawat, Appl. Phys. Lett. 61 (**6**) (1992)
[26] K. Pangal, J. C. Sturm, S. Wagner and T. H. Büyüklimanli, J. Appl. Phys **85**,3, (1999).
[27] J. Dong, D. A. Drabold, Phys. Rev. **B 54**, 10284 (1996).